Available online at www.sciencedirect.com
SCIENCE DIRECT®
Earth and Planetary Science Letters 240 (2005) 559–572
EPSL
www.elsevier.com/locate/epsl

Evidence for a mantle component shown by rare gases, C and N isotopes in polycrystalline diamonds from Orapa (Botswana)

Cécile Gautheron [a,*], Pierre Cartigny [b], Manuel Moreira [a], Jeff. W. Harris [c], Claude J. Allègre [a]

[a] *Laboratoire de Géochimie et Cosmochimie (UMR 7579 CNRS), Institut de Physique du Globe de Paris, Université Paris 7, 4 place Jussieu 75252 Paris, Cedex 05, France*
[b] *Laboratoire de Géochimie des Isotopes Stables (UMR 7047 CNRS), Institut de Physique du Globe de Paris, Université Paris 7, 4 place Jussieu 75252 Paris, Cedex 05, France*
[c] *Division of Earth Sciences, Centre for GeoSciences, Gregory Building, University of Glasgow, Glasgow G12 8QQ, Scotland, UK*

Received 24 February 2005; received in revised form 22 September 2005; accepted 22 September 2005
Available online 16 November 2005
Editor: K. Farley

Abstract

In an attempt to constrain the origin of polycrystalline diamond, combined analyses of rare gases and carbon and nitrogen isotopes were performed on six such diamonds from Orapa (Botswana). Helium shows radiogenic isotopic ratios of R/Ra = 0.14–1.29, while the neon ratios ($^{21}Ne/^{22}Ne$ of up to 0.0534) reflect a component from mantle, nucleogenic and atmospheric sources. $^{40}Ar/^{36}Ar$ ratios of between 477 and 6056 are consistent with this interpretation. The ($^{129}Xe/^{130}Xe$) isotopic ratios range between 6.54 and 6.91 and the lower values indicate an atmospheric component. The He, Ne, Ar and Xe isotopic compositions and the Xe isotopic pattern are clear evidence for a mantle component rather than a crustal one in the source of the polycrystalline diamonds from Orapa. The $\delta^{13}C$ and $\delta^{15}N$ isotopic values of −1.04 to −9.79‰ and +4.5 to +15.5‰ respectively, lie within the range of values obtained from the monocrystalline diamonds at that mine. Additionally, this work reveals that polycrystalline diamonds may not be the most appropriate samples to study if the aim is to consider the compositional evolution of rare gases through time. Our data shows that after crystallization, the polycrystalline diamonds undergo both gas loss (that is more significant for the lighter rare gases such as He and Ne) and secondary processes (such as radiogenic, nucleogenic and fissiogenic, as well as atmospheric contamination). Finally, if polycrystalline diamonds sampled an old mantle (1–3.2 Ga), the determined Xe isotopic signatures, which are similar to present MORB mantle – no fissiogenic Xe from fission of ^{238}U being detectable – imply either that Xe isotopic ratios have not evolved within the convective mantle since diamond crystallization, or that these diamonds are actually much younger.

Keywords: rare gases; carbon; nitrogen; polycrystalline diamonds; Orapa

1. Introduction

Rare gas studies provide important constraints on the origin and evolution of the atmosphere and mantle reservoirs of our planet. Helium isotopic systematics of mantle rocks allows Earth mantle reservoirs to be distinguished. For instance, the relatively constant

* Corresponding author. Now UMR Interactions et Dynamique des Environnements de Surface, UMR 8148 CNRS, Université Paris 11–Orsay, 91405 Orsay Cedex, France. Tel.: +33 1 69 15 67 83; fax: +33 1 69 15 48 82.
E-mail address: gautheron@geol.u-psud.fr (C. Gautheron).

0012-821X/$ - see front matter © 2005 Elsevier B.V. All rights reserved.
doi:10.1016/j.epsl.2005.09.060

$^4He/^3He$ of 90,000 ± 10,000 or R/Ra of 8 ± 1, measured in mid-Oceanic Ridge Basalts (MORB) [1], has been interpreted to represent a degassed reservoir assumed to be the upper mantle [2]. The subcontinental lithospheric mantle (SCLM) presents a more radiogenic helium isotopic ratio ($^4He/^3He$ of 116,000 ± 15,500 or R/Ra = 6.1 ± 0.9 [3]), than the surrounding upper mantle. However, the SCLM remains poorly constrained for other rare gases. Also, almost no data on the Archean mantle is available and its evolution through time remains to be established. As diamonds derive from the subcontinental mantle and have different genesis ages [4], they may provide constraints on rare gas evolution. The diamond work so far completed suggests that opaque and/or fibrous cube diamonds have helium isotopic ratios ($^4He/^3He$ = 119,000 ± 20,000 or R/Ra = 6.1 ± 1.2 [5]), typical of the SCLM, yet may have a genesis age contemporaneous with the (proto-) kimberlite magmatism [6,7]. For typical monocrystalline and polycrystalline diamond, ancient SCLM rare gas signatures [8–10] have been determined. These primary signatures from diamond may be affected by secondary processes which may dramatically influence the final rare gas value. For example, in polycrystalline diamonds particularly, where the aggregated nature of the material (see [11]) has the potential to bear large rare gas contents, secondary helium isotopes can be produced by nucleogenic, cosmogenic, radiogenic and α-implantation processes [12–15]. Accordingly, accessing the "pristine" trapped helium signature is difficult and no clear conclusion has yet been obtained. In addition, whether these diamonds formed both in the same host rocks and at the same time as monocrystalline diamonds remain to be established. With the other rare gas isotopes, such as neon, argon and xenon, only small numbers of analyses have been completed and for these elements, available data often have a scatter as a consequence of small sample sizes, low rare gas contents, or an obvious atmospheric contamination [5,9].

In the present study, six polycrystalline (aggregated) diamonds of >2cm size were analyzed from the Orapa mine in Botswana with four of them belonging either to the peridotitic or eclogitic paragenesis. The samples were further analyzed for their C and N isotopes and N contents and the results allow, in light of available data on monocrystalline diamonds from the same mine, to discuss their possible relationships.

2. Sample location and analytical procedures

Orapa is the largest of 23 pipes found in northeastern Botswana, 250 km west of Francistown, and is a Group I kimberlite emplaced 93.1 Ma ago [16]. With the present six samples, silicate inclusions both on the surfaces and within the stones defined four samples to a paragenesis. ORPC1 to 3 contained orange eclogitic garnets while ORPC4 contained peridotitic emerald–green diopside inclusions (see Table 1). ORPC5 and 6 have much smaller diamond crystallites and are of unknown paragenesis. For this study, the diamonds were broken and selected pieces, weighing between 0.43 and 0.81 g, cleaned with double-distilled water, ethanol and acetone. Because sample ORPC4 #1 was particularly mineral inclusion-rich, an HF 7N leaching procedure was adopted to dissolve surface inclusions. With ORPC4, a second piece (ORPC4 #2), free of visible diopside inclusions was taken. Although apparently free of surface inclusions, ORPC5 and 6 were leached for 45 min with HF 7N in an ultrasonic bath, and 3 h in a 27 N (2 cc) HF and 16 N (2 cc) HNO_3 mixture on a hot plate (140–200 °C), then rinsed with double-distilled water, ethanol and acetone. With these

Table 1
Description of samples, number of strokes and weight of diamonds

Samples	Description	Strokes	Weight (g)
ORPC1 step1	Bottom center right framesite	300	
ORPC1 step2		350	
ORPC1 step3		350	
ORPC1 Total		**1000**	**0.4292**
ORPC2 step1	Center	350	
ORPC2 step2		350	
ORPC2 step3		450	
ORPC2 Total		**1150**	**0.6453**
ORPC3 step1	Less crystallized	50	
ORPC3 step2		150	
ORPC3 step3		200	
ORPC3 Total		**400**	**0.5498**
ORPC4 #1 step1	Traces of diopside	150	
ORPC4 #1 step2		200	
ORPC4 #1 step3		150	
ORPC4 #1 step4		300	
ORPC4 #1 Total		**800**	**0.6907**
ORPC4 #2 step1	2 pieces from the middle, no trace of diopside	300	
ORPC4 #2 step2		300	
ORPC4 #2 step3		350	
ORPC4 #2 Total		**950**	**0.2272**
ORPC5 step1	1 piece	500	
ORPC5 step2		400	
ORPC5 step3		450	
ORPC5 Total		**1350**	**0.5690**
ORPC6 step1	1 piece	500	
ORPC6 step2		450	
ORPC6 step3		400	
ORPC6 Total		**1350**	**0.8068**

procedures the diamonds were cleaned of visible secondary mineral inclusions.

Rare gases were extracted using a step-crushing procedure as opposed to step-heating. This procedure was adopted because step-crushing permitted access to rare gases contained within fluid inclusions and such gases are usually less affected by radiogenic, nucleogenic and fissiogenic production in the diamond matrix. Prior to an analysis, diamonds and crusher were baked overnight at 130 °C under vacuum to remove possible atmospheric rare gases trapped on their surfaces. The rare gas extraction used three or four steps of crushing, where the number of crushing strokes in a step varies between 150 and 500 (see Table 1).

Rare gases were purified, separated, and analyzed with the glass mass spectrometer ARESIBO I equipped with a Faraday cup and an ion-counting system. Helium and neon were first separated from other rare gases using a charcoal trap cooled at liquid nitrogen temperature, and purified with a SAES 707 getter at room temperature. Helium and neon were then sorbed on a cryogenic trap at 13 K. At 30 K helium was released and introduced into the mass spectrometer. At 70 K, neon was released and analyzed. The isotopic ratios of blanks are similar to atmospheric ones. ^{4}He and ^{22}Ne blanks were 8.2×10^{-9} and $2–5\times10^{-13}$ ccSTP respectively (for clarity, the percentage of ^{22}Ne blank are reported in Table 2). Helium and neon concentrations and isotopic ratios were corrected from blanks. Special care was taken during neon analyses so that the amount of Ar and CO_2 always remain similar in blanks, standards and samples. The $^{40}Ar^{2+}/^{40}Ar^{+}$ and $^{44}CO_2^{2+}/^{44}CO_2^{+}$ ratios were respectively 0.15 and 0.075. During the analyses, only step 2 for ORPC6 had a high $^{44}CO_2$ level (4 times higher than average) and for this reason, this value was excluded. During helium and

Table 2
Concentration and isotopic ratios of helium, neon and argon obtained by crushing

Samples	^{4}He (10^{-8})	R/Ra	Blank ^{22}Ne proportion	^{22}Ne (10^{-12})	^{20}Ne/^{22}Ne	^{21}Ne/^{22}Ne	^{36}Ar (10^{-10})	^{40}Ar/^{36}Ar
ORPC1 step1	22.4 ± 0.007	0.97 ± 0.03	0.11	8.9 ± 0.08	9.86 ± 0.03	0.0302 ± 0.0002	3.2 ± 0.3	3747 ± 30
ORPC1 step2	14.1 ± 0.007	0.45 ± 0.04	0.41	1.6 ± 0.02	9.83 ± 0.08	0.0322 ± 0.0006	0.5 ± 0.05	6982 ± 57
ORPC1 step3	9.66 ± 0.003	0.31 ± 0.05	0.45	1.4 ± 0.02	9.89 ± 0.09	0.0332 ± 0.0010	0.5 ± 0.05	3653 ± 30
ORPC1 Total	**46.2 ± 0.017**	**0.54 ± 0.06**		**12 ± 0.12**	**9.86 ± 0.05**	**0.0308 ± 0.0004**	**4.1 ± 0.3**	**4092 ± 33**
ORPC2 step1	8.14 ± 0.002	1.72 ± 0.07	0.01	133 ± 2	9.76 ± 0.02	0.0290 ± 0.0001	36.4 ± 3.6	424 ± 3
ORPC2 step2	3.37 ± 0.002	1.12 ± 0.12	0.37	1.6 ± 0.02	9.84 ± 0.05	0.0303 ± 0.0022	0.5 ± 0.1	2569 ± 21
ORPC2 step3	3.35 ± 0.003	0.89 ± 0.10	0.41	1.3 ± 0.02	9.75 ± 0.06	0.0300 ± 0.0026	0.7 ± 0.1	1755 ± 21
ORPC2 Total	**14.9 ± 0.007**	**1.29 ± 0.11**		**136 ± 2**	**9.76 ± 0.02**	**0.0290 ± 0.0002**	**37.6 ± 4**	**477 ± 4**
ORPC3 step1	1.53 ± 0.316	1.11 ± 0.30	0.50	0.8 ± 0.02	7.86 ± 0.12	0.0327 ± 0.0013	14.2 ± 1.4	320 ± 3
ORPC3 step2	13.2 ± 0.006	0.40 ± 0.03	0.23	3.4 ± 0.04	9.87 ± 0.04	0.0323 ± 0.0003	5.7 ± 0.6	694 ± 7
ORPC3 step3	15.4 ± 0.006	0.39 ± 0.04	0.30	2.4 ± 0.05	9.94 ± 0.37	0.0376 ± 0.0088	1.2 ± 0.1	2084 ± 30
ORPC3 Total	**30.1 ± 0.328**	**0.41 ± 0.04**		**6.7 ± 0.11**	**9.63 ± 0.17**	**0.0342 ± 0.0035**	**21.1 ± 1**	**518 ± 5**
ORPC4 #1 step1	21.4 ± 0.005	1.12 ± 0.03	0.01	96 ± 1.2	9.82 ± 0.02	0.0324 ± 0.0001	22 ± 2	4849 ± 40
ORPC4 #1 step2	21.6 ± 0.006	0.95 ± 0.02	0.04	20 ± 0.3	10.0 ± 0.03	0.0437 ± 0.0001	4.7 ± 0.5	15,698 ± 129
ORPC4 #1 step3	8.90 ± 0.007	0.89 ± 0.06	0.12	5.7 ± 0.08	9.98 ± 0.03	0.0469 ± 0.0006	b.p.[a]	b.p.
ORPC4 #1 step4	14.3 ± 0.003	0.78 ± 0.04	0.12	6.0 ± 0.08	10.12 ± 0.03	0.0534 ± 0.0007	2.6 ± 0.3	16,805 ± 138
ORPC4 #1 Total	**66.2 ± 0.022**	**0.94 ± 0.04**		**128 ± 1.7**	**9.87 ± 0.02**	**0.0358 ± 0.0002**	**29.4 ± 1.8**	**5399 ± 63**
ORPC4 #2 step1	45.6 ± 0.002	0.30 ± 0.04	0.32	7.1 ± 0.2	10.01 ± 0.05	0.0346 ± 0.0001	3 ± 0.02	2000 ± 7
ORPC4 #2 step2	33.8 ± 0.001	0.16 ± 0.04	0.45	2.1 ± 0.06	9.90 ± 0.09	0.0362 ± 0.0001	0.8 ± 0.01	3384 ± 12
ORPC4 #2 step3	29.0 ± 0.001	0.07 ± 0.04	0.55	1.4 ± 0.04	10.01 ± 0.14	0.0305 ± 0.0001	0.5 ± 0.01	2869 ± 10
ORPC4 #2 Total	**109 ± 0.004**	**0.14 ± 0.05**		**10.6 ± 0.3**	**9.99 ± 0.07**	**0.0344 ± 0.0001**	**4.3 ± 0.02**	**2346 ± 8**
ORPC5 step1	5.12 ± 0.006	0.84 ± 0.07	0.11	4.6 ± 0.02	9.90 ± 0.05	0.0295 ± 0.0005	2.3 ± 0.003	2782 ± 67.32
ORPC5 step2	12.0 ± 0.015	1.15 ± 0.08	0.14	3.5 ± 0.02	9.91 ± 0.03	0.0302 ± 0.0003	2.2 ± 0.005	7140 ± 190
ORPC5 step3	4.67 ± 0.006	0.48 ± 0.07	0.46	0.7 ± 0.02	9.95 ± 0.07	0.0319 ± 0.0008	0.4 ± 0.001	11,668 ± 253
ORPC5 Total	**21.8 ± 0.027**	**0.83 ± 0.08**		**8.7 ± 0.06**	**9.90 ± 0.04**	**0.0300 ± 0.0005**	**4.9 ± 0.003**	**5446 ± 137**
ORPC6 step1	32.3 ± 0.562	0.86 ± 0.06	0.05	7.8 ± 0.03	10.01 ± 0.03	0.0300 ± 0.0003	4.2 ± 0.01	3790 ± 80
ORPC6 step2	12.8 ± 0.223	0.70 ± 0.04	pb[b]	pb[b]	pb[b]	pb[b]	4.4 ± 0.01	7116 ± 195
ORPC6 step3	9.25 ± 0.161	0.19 ± 0.02	0.51	0.4 ± 0.01	10.64 ± 0.16	0.0406 ± 0.0025	2.5 ± 0.004	7994 ± 161
ORPC6 Total	**54.3 ± 0.936**	**0.52 ± 0.04**		**8.2 ± 0.04**	**10.04 ± 0.04**	**0.0306 ± 0.0004**	**11.1 ± 0.01**	**6056 ± 144**
Air[c]		**1**			**9.8**	**0.0290**		**295.5**

The ^{4}He, ^{22}Ne and ^{36}Ar are given in ccSTP/g. The errors are given as 1σ.

[a] Blank problem.

[b] Ar and CO_2 level 4 times higher than during blank, standard and the other steps.

[c] Air value are taken from [21].

neon analysis, the charcoal trap was warmed to room temperature and desorbed gas was purified using two hot titanium getters (800 °C). Argon, krypton and xenon were then sorbed on the cryogenic trap at 70 K, then desorbed successively and introduced in the mass spectrometer.

For each sample, the diamond powder resulting from crushing was usually <500 μm. Larger grains were rare, but were recovered after sieving and analyzed for carbon and nitrogen isotopic composition. Selecting the largest grains ensures that no metal fragment is present from the crusher or the ball used for crushing (which may occur within the fine-grained diamond powder). Several grains were grouped, their mass ranging from 0.47 to 1.71 mg, wrapped in platinum foil, cleaned and analyzed for N concentration, N and C isotopes using well established techniques [17,18]. Nitrogen and carbon isotopic compositions are expressed using the conventional δ-notation (where for nitrogen $\delta^{15}N = [(^{15}N/^{14}N_{sample}/^{15}N/^{14}N_{Air} - 1) \times 1000]$); values for carbon were normalized relative to the PDB standard. Accuracy for nitrogen concentration, nitrogen and carbon isotopic compositions were ±5%, ±0.5‰, ±0.1‰ (2σ) respectively.

3. Results

3.1. Rare gases concentrations and isotopic ratios

Table 1 reports a brief description as well as analytical conditions applied for each of the crushing steps. Rare gas concentrations and isotopic compositions are reported in Tables 2 and 3. In this work, "total" isotopic ratio, refers to the weighted isotopic ratio calculated by summing the steps using a mass balance law. Because the $^{38}Ar/^{36}Ar$ and the Kr isotopic ratios are indistin-

Table 3
Concentrations and isotopic compositions of krypton and xenon

Samples	^{84}Kr (10^{-12})	^{130}Xe (10^{-14})	$^{128}Xe/^{130}Xe$	$^{129}Xe/^{130}Xe$	$^{131}Xe/^{130}Xe$	$^{132}Xe/^{130}Xe$	$^{134}Xe/^{130}Xe$	$^{136}Xe/^{130}Xe$
ORPC1 step1	10.3 ± 0.2	17.8 ± 0.4	0.47 ± 0.01	6.78 ± 0.05	5.27 ± 0.03	6.69 ± 0.04	2.62 ± 0.02	2.26 ± 0.01
ORPC1 step2	3.0 ± 0.1	8.9 ± 0.4	0.47 ± 0.01	6.64 ± 0.10	5.23 ± 0.07	6.67 ± 0.10	2.59 ± 0.03	2.25 ± 0.03
ORPC1 step3	1.5 ± 0.1	5.1 ± 0.2	0.47 ± 0.01	6.81 ± 0.14	5.26 ± 0.10	6.71 ± 0.16	2.56 ± 0.04	2.21 ± 0.04
ORPC1 Total	**14.8 ± 0.4**	**31.8 ± 1.0**	**0.47 ± 0.01**	**6.75 ± 0.08**	**5.26 ± 0.05**	**6.69 ± 0.08**	**2.60 ± 0.05**	**2.25 ± 0.02**
ORPC2 step1	98.7 ± 1.6	100 ± 5.2	0.48 ± 0.01	6.52 ± 0.04	5.22 ± 0.02	6.63 ± 0.04	2.59 ± 0.01	2.19 ± 0.01
ORPC2 step2	2.4 ± 0.1	7.7 ± 0.4	0.46 ± 0.01	6.71 ± 0.06	5.32 ± 0.04	6.75 ± 0.06	2.65 ± 0.02	2.22 ± 0.02
ORPC2 step3	2.6 ± 0.1	7.1 ± 0.4	0.47 ± 0.01	6.62 ± 0.07	5.27 ± 0.05	6.72 ± 0.08	2.62 ± 0.03	2.25 ± 0.02
ORPC2 Total	**103.7 ± 1.8**	**114.8 ± 6.0**	**0.47 ± 0.01**	**6.54 ± 0.04**	**5.23 ± 0.03**	**6.64 ± 0.04**	**2.59 ± 0.01**	**2.19 ± 0.01**
ORPC3 step1	20.7 ± 1.6	20.4 ± 0.8	0.47 ± 0.01	6.59 ± 0.06	5.24 ± 0.04	6.65 ± 0.06	2.55 ± 0.03	2.15 ± 0.02
ORPC3 step2	5.6 ± 2	15.9 ± 1.1	0.51 ± 0.01	6.73 ± 0.08	5.25 ± 0.06	6.64 ± 0.08	2.56 ± 0.03	2.19 ± 0.03
ORPC3 step3	3.1 ± 2	b.p.[a]		n.m.[b]	n.m.	n.m.	n.m.	n.m.
ORPC3 Total	**29.4 ± 2**	**36.3 ± 1.9**	**0.49 ± 0.01**	**6.66 ± 0.07**	**5.25 ± 0.05**	**6.65 ± 0.07**	**2.56 ± 0.03**	**2.17 ± 0.02**
ORPC4 #1 step1	67.1 ± 1.1	79.2 ± 1.5	0.48 ± 0.01	6.53 ± 0.04	5.19 ± 0.02	6.60 ± 0.04	2.66 ± 0.01	2.27 ± 0.01
ORPC4 #1 step2	20.1 ± 0.4	43.4 ± 0.9	0.47 ± 0.01	6.66 ± 0.05	5.25 ± 0.03	6.71 ± 0.04	2.72 ± 0.01	2.37 ± 0.01
ORPC4 #1 step3	3.4 ± 0.23	14.4 ± 0.3	0.47 ± 0.01	6.64 ± 0.06	5.24 ± 0.04	6.67 ± 0.06	2.73 ± 0.01	2.40 ± 0.02
ORPC4 #1 step4	9.6 ± 0.83	23.8 ± 0.5	0.48 ± 0.01	6.62 ± 0.04	5.19 ± 0.02	6.66 ± 0.04	2.71 ± 0.01	2.35 ± 0.01
ORPC4 #1 Total	**100.1 ± 2.56**	**160.8 ± 3.2**	**0.47 ± 0.01**	**6.59 ± 0.04**	**5.21 ± 0.03**	**6.65 ± 0.04**	**2.69 ± 0.01**	**2.32 ± 0.01**
ORPC4 #2 step1	20.1 ± 0.24	43.8 ± 1.1	0.48 ± 0.01	6.64 ± 0.05	5.30 ± 0.04	6.71 ± 0.06	2.62 ± 0.02	2.26 ± 0.02
ORPC4 #2 step2	3.8 ± 0.08	15.3 ± 0.37	0.46 ± 0.01	6.70 ± 0.09	5.29 ± 0.07	6.73 ± 0.09	2.65 ± 0.03	2.26 ± 0.03
ORPC4 #2 step3	2.2 ± 0.05	9.1 ± 0.27	0.48 ± 0.01	6.76 ± 0.11	5.36 ± 0.08	6.88 ± 0.11	2.66 ± 0.05	2.31 ± 0.04
ORPC4 #2 Total	**26.0 ± 0.37**	**68.2 ± 1.74**	**0.47 ± 0.01**	**6.67 ± 0.07**	**5.31 ± 0.05**	**6.74 ± 0.07**	**2.63 ± 0.03**	**2.27 ± 0.02**
ORPC5 step1	7.6 ± 0.24	10.3 ± 0.6	0.47 ± 0.01	6.75 ± 0.13	5.29 ± 0.09	6.71 ± 0.10	2.69 ± 0.05	2.29 ± 0.03
ORPC5 step2	7.1 ± 0.23	10.1 ± 0.4	0.48 ± 0.01	7.02 ± 0.11	5.33 ± 0.06	6.76 ± 0.07	2.69 ± 0.04	2.34 ± 0.02
ORPC5 step3	1.4 ± 0.22	3.9 ± 0.2	0.45 ± 0.01	7.00 ± 0.11	5.27 ± 0.05	6.68 ± 0.08	2.66 ± 0.05	2.39 ± 0.04
ORPC5 Total	**16.1 ± 0.69**	**24.1 ± 1.2**	**0.47 ± 0.01**	**6.91 ± 0.12**	**5.30 ± 0.07**	**6.72 ± 0.09**	**2.68 ± 0.05**	**2.33 ± 0.03**
ORPC6 step1	15.2 ± 0.5	23.3 ± 0.8	0.47 ± 0.01	6.67 ± 0.10	5.21 ± 0.04	6.62 ± 0.06	2.54 ± 0.04	2.20 ± 0.01
ORPC6 step2	2.6 ± 0.1	7 ± 0.2	0.47 ± 0.01	6.60 ± 0.10	5.31 ± 0.08	6.70 ± 0.10	2.57 ± 0.04	2.27 ± 0.03
ORPC6 step3	1.2 ± 0.1	4 ± 0.3	0.48 ± 0.01	6.68 ± 0.13	5.26 ± 0.07	6.69 ± 0.09	2.61 ± 0.05	2.26 ± 0.03
ORPC6 Total	**19.0 ± 0.7**	**34.3 ± 1.3**	**0.47 ± 0.01**	**6.66 ± 0.10**	**5.24 ± 0.05**	**6.64 ± 0.07**	**2.56 ± 0.04**	**2.22 ± 0.02**
Air[c]			**0.47**	**6.50**	**5.21**	**6.61**	**2.56**	**2.18**

^{84}Kr and ^{132}Xe are given in ccSTP/g respectively. The errors are given in 1σ.

[a] Blank problem.

[b] Not measured.

[c] Air value are taken from [21].

guishable from the atmospheric ratios, these are neither reported nor discussed later.

Total helium concentrations vary between 15 and 109×10^{-8} ccSTP/g. In general, these values are lower than previous measurements on other polycrystalline diamonds from Orapa (^{4}He between 0.03 and 70×10^{-6} ccSTP/g by crushing [14] and between 0.03 and 66×10^{-6} ccSTP/g by graphitization [14]). The values are also lower when compared with polycrystalline diamonds from the Jwaneng kimberlite (Botswana) with ^{4}He between 0.03 and 4×10^{-6} ccSTP/g by crushing [15] and between 55 and 173×10^{-6} ccSTP/g by graphitization [15,19]. These differences may reflect real variations in helium concentrations but are more likely induced by the rare gas extraction method. For diamonds, Kurz et al. [14] have found that their stepwise crushing seems to release ~10% of the total helium concentration.

Orapa diamonds display very high ^{4}He/^{3}He isotopic ratios (560,000–5,023,000) compared to the mean MORB value (^{4}He/^{3}He = 90,000 ± 10,000). For convenience, the helium isotopic ratio is normalized to air and expressed as R/Ra (with Ra = 1.384×10^{-6}). Thus, the R/Ra ratios for the diamonds vary between 0.14 and 1.29 (other relevant R/Ra ratios are: radiogenic ~0, AIR ≡ 1, SCLM ~ 6 and MORB ~ 8). Compared to the sub-oceanic mantle these ratios are radiogenic, but are within the range of published data on polycrystalline diamonds from Orapa (R/Ra = 0.02–4.6 [14,15,19]). They are however distinct from cubic diamonds from kimberlite (R/Ra = 3–9.3 [5,20]).

Total ^{22}Ne concentrations range between 7 and 136×10^{-12} ccSTP/g. These values lie within both the range given by polycrystalline diamonds from Jwaneng [15] and cubic/fibrous diamonds from Orapa [5,9]. Total ^{20}Ne/^{22}Ne ratios vary between 9.63 and 10.04 and total ^{21}Ne/^{22}Ne ratios range from 0.029 to 0.036. The variation of the ^{20}Ne/^{22}Ne ratio with steps is small compared to the variation of the ^{21}Ne/^{22}Ne ratio. Like ^{4}He/^{3}He, ^{21}Ne/^{22}Ne isotopic ratios increase as a function of the number of strokes, while the ^{20}Ne/^{22}Ne ratio is relatively constant. Total ratios are generally close to atmosphere (Fig. 1; ^{20}Ne/^{22}Ne = 9.8 and ^{21}Ne/^{22}Ne = 0.029 [21]). Additionally, on Fig. 1, where the MORB and the OIB fields are shown [22–26], one step of sample ORPC6 (Fig. 1A, see also Table 2) displays a MORB-like signature. The remaining crushing steps/samples show a nucleogenic ^{21}Ne/^{22}Ne ratio, which is usually identified within the second or third crushing step.

Total ^{36}Ar concentrations vary from 4 to 38×10^{-10} ccSTP/g, lying within the lowermost range of the measured values for polycrystalline diamonds from

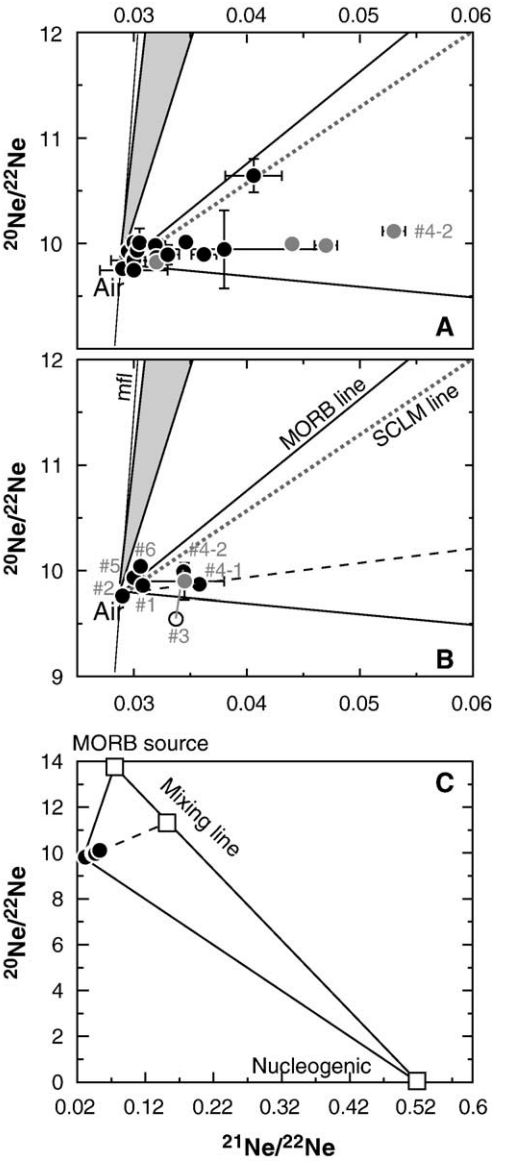

Fig. 1. The Ne isotope results in diagram (A) shows all the step-crushing results, while the weighted averages of the six specimens can be seen in diagram (B). Also defined (labeled in diagram B) are the mass fractionation line (mfl), the MORB line defined by [22], the subcontinental lithospheric mantle line (SCLM) [46] and the primitive OIB field (gray) [23–26]. First step of sample ORPC3 shows a low ^{20}Ne/^{22}Ne ratio. The weighted average for sample ORPC3 is plotted both considering (open symbol) and neglecting (filled symbol) the low ^{20}Ne/^{22}Ne ratio measured in the first step of crushing. The samples fall on a horizontal line, showing ^{21}Ne excess compared to air, as shown in diagram (C) (for clarification only sample ORPC4 steps being represented). This figure illustrates that the polycrystalline diamonds from Orapa are characterized by mixing between a MORB mantle source and a nucleogenic component [33,60], followed by air contamination (dashed line in panels B and C). Variations in mantle/nucleogenic proportions are likely, but, because of the strong atmospheric contamination, are only poorly resolvable.

both Orapa [19] and Jwaneng [15]. However, the ^{36}Ar concentrations measured in this study are higher than for cubic diamonds [5]. The total $^{40}Ar/^{36}Ar$ isotopic ratios are between 477 (ORPC2) and 6056 (ORPC6) (see Fig. 2) and again, the results are similar to those of [19] and [15]. Sample ORPC4 #1 step 4 shows a $^{40}Ar/^{36}Ar$ ratio up to 16,805 indicating significant radiogenic ^{40}Ar.

Total ^{84}Kr concentrations vary between 15 and 104×10^{-12} ccSTP/g and are similar to both Jwaneng polycrystalline diamonds [15] and cubic kimberlite-related diamonds [9]. Total ^{130}Xe concentrations range between 24 and 161×10^{-14} ccSTP/g, which is similar to that for Jwaneng polycrystalline diamonds [15] but lower than for cubic diamonds (i.e. coat+core [9]). Total $^{129}Xe/^{130}Xe$ ratios vary between 6.54 ± 0.04 and 6.91 ± 0.12 and thus, show significant anomalies compared to the atmospheric value of 6.50. As illustrated in Fig. 3A and B, the present total $^{129}Xe/^{130}Xe$ and $^{136}Xe/^{130}Xe$ data actually plot close to the MORB line. Additionally, Fig. 4 shows the xenon pattern of samples ORPC4 #1 and ORPC5 compared to MORB and crustal samples.

3.2. Carbon and Nitrogen stable isotope compositions

C and N isotopic compositions and nitrogen concentrations are reported in Table 4. Diamond $\delta^{13}C$ values range between −21.04 and −9.79‰ and $\delta^{15}N$ values between +4.5 and +15.5‰. As illustrated in Fig. 5, the present $\delta^{13}C$–$\delta^{15}N$ data strongly overlap with previous diamond studies from the same mine, including eclogitic and peridotitic monocrystalline diamonds [27,28]. Nitrogen concentration varies between 69 and 1973 ppm, the highest N concentration being associated with the highest $\delta^{13}C$ value. For a given $\delta^{13}C$, nitrogen concentrations of polycrystalline diamonds are slightly higher than their monocrystal counterparts, but the decrease in diamond N concentration with decreasing $\delta^{13}C$ value identified among Orapa and worldwide dataset is supported by the present data [18].

4. Discussions and interpretations

In diamond, nitrogen atoms are trapped in the diamond crystal lattice substituting for carbon atoms [29]. The good correlation between N contents determined by IR-spectroscopy and bulk combustion [30] suggests that none, or very limited amounts of nitrogen, occur as fluid inclusions. The situation is much more complex for rare gases. Due to their physical and chemical properties, rare gases within a diamond matrix may be located either along grain boundaries, in fluid inclusions, within mineral inclusions, adsorbed on the diamond surface or exist within the actual diamond matrix. In addition, the aggregated nature of polycrystalline diamond makes rare gases potentially sensitive to both air contamination and diffusion loss after crystallization; see [31,32]. The presence of diopside and garnet inclusions (enriched in U, Th and K relative to diamond, [19]) makes polycrystalline diamonds potentially susceptible to post-crystallization secondary production of rare gases (in the mineral inclusions) by either implantation, radiogenic, nucleogenic or fissiogenic processes. Based on our results, we identify three different processes that may control the rare gas elemental and isotopic compositions: (1) trapping of mantle gas (2) radiogenic–nucleogenic and fissiogenic production before and after diamond crystallization followed by air contamination and (3) loss after diamond crystallization.

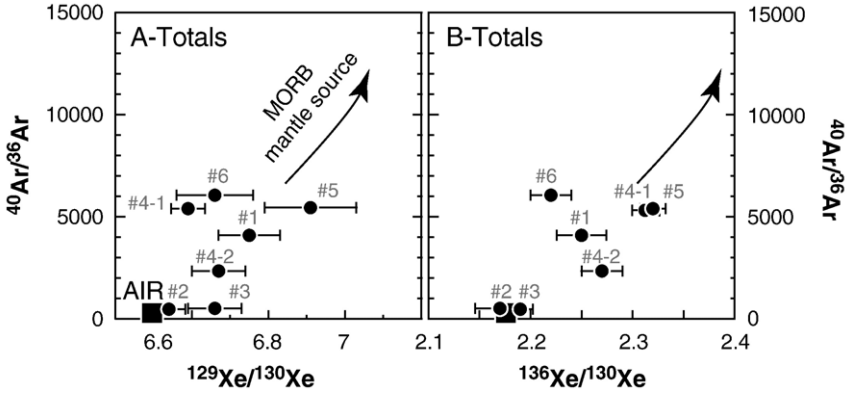

Fig. 2. The plots of $^{40}Ar/^{36}Ar$ with $^{129}Xe/^{130}Xe$ (A) and with $^{136}Xe/^{130}Xe$ (B) are the weighted average of the step-crushing experiments. The atmospheric value is shown as a black square. These data show clearly a mixing between air and a mantle source, the dispersion reflecting the complex story of the polycrystalline diamonds from Orapa.

4.1. Mantle signature in the source of the polycrystalline diamonds

The higher R/Ra ratio in the diamonds, relative to that of the crust (R ≈ 0.02 Ra, [33]) strongly indicates the presence of mantle ^{3}He. Similarly, neon and argon isotopic ratios show a mantle component (combined with air and radiogenic–nucleogenic components), as illustrated by Figs. 1 and 2. Nevertheless, most Ne results show the influence of pre- and post-crystallization nucleogenic production (see Section 4.2.). The Ne isotopic results imply a mantle-derived contribution (see Fig. 1C) and one crushing step (ORPC 6 step 3, see Table 2) falls, within errors, on the MORB line (Fig. 1A). In this study, xenon isotopic ratios are all close to MORB values (see Fig. 3 [34, 35]). In particular, the ^{129}Xe/^{130}Xe and ^{136}Xe/^{130}Xe ratios are clearly higher than air and correlated in a manner very similar to MORBs (Fig. 3A and B). So, xenon isotopic ratios are key evidence in supporting the crystallization of eclogitic, peridotitic and unknown paragenesis diamonds from a mantle-related fluid, and will be the main focus of discussion in this section.

This conclusion differs from that of Honda and collaborators [15], who proposed that, within polycrystalline diamonds from the Jwaneng mine, the Ne and Xe isotopes are of crustal origin rather than mantle derived. This conclusion was based on two observations: (1) the absence of a mantle neon signature and (2) that ^{131}Xe/^{130}Xe values were above the MORB range when compared to ^{129}Xe/^{130}Xe or ^{136}Xe/^{130}Xe. In the second observation, they noted that thermal and epithermal neutron capture reactions by the Tellurium isotope ^{128}Te would produce ^{129}I through β decays [36,37], while neutron capture by ^{130}Te would produce ^{131}Xe. They further argued that (1) in mantle rocks or in mineral inclusions in diamond, ^{128}Te and ^{130}Te concentrations are too small to yield any measurable amount of ^{129,} ^{131}Xe [38], and (2) a correlation between ^{131}Xe/^{130}Xe and ^{129}Xe/^{130}Xe was observed in crustal rocks [39].

Although our view differs, the present Xe results on Orapa diamonds are actually very similar to Jwaneng and both fall on the MORB line in the ^{129}Xe/^{130}Xe vs. ^{136}Xe/^{130}Xe diagram. The only discrepancy lies in the

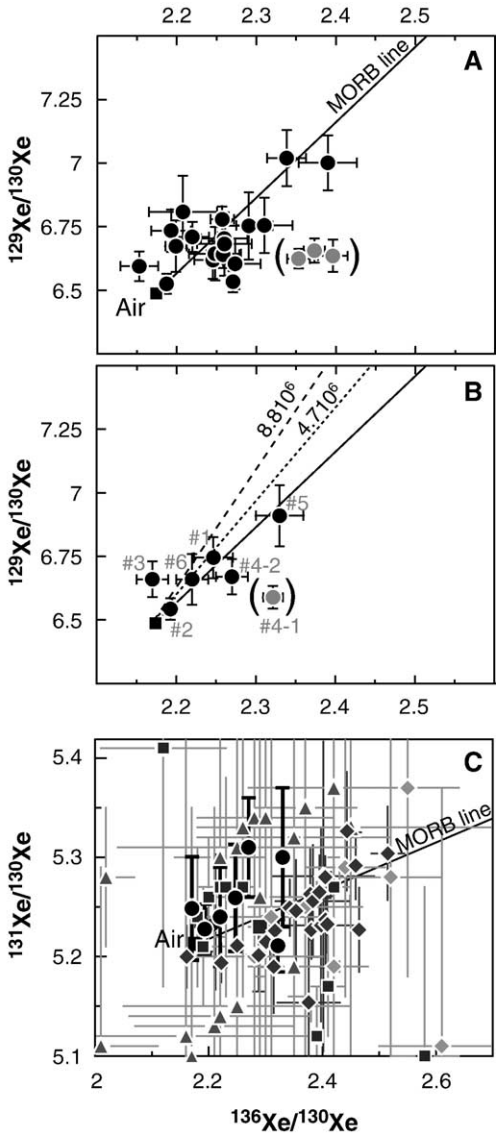

Fig. 3. Xenon data reported in diagrams (A and B) as ^{129}Xe/^{130}Xe vs. ^{136}Xe/^{130}Xe. All steps are plotted in diagram (A) and weighted average in diagram (B). Also shown are the MORB line [34,35] and mixing lines between air and the calculated mantle source 3 Ga ago for two different ^{238}U/^{130}Xe ratios. In this calculation, the ^{238}U/^{130}Xe ratio remains the least constrained parameter. A range of values between 4.7×10^6 and 8.8×10^6, deduced from the study of MORB, has been assumed [61,62]. The present-day value of ^{136}Xe/^{130}Xe is taken at 2.72 [62]. For example, 3 Ga ago, the mantle ^{136}Xe/^{130}Xe ratio is calculated to be 2.53 and 2.62 for a ^{238}U/^{130}Xe of 8.8×10^6 and 4.7×10^6 respectively. Given the error bars, only the line for the ^{238}U/^{130}Xe of 8.8×10^6 is significantly different from the present MORB line. Taking more appropriate values for the subcontinental lithospheric mantle (U content of 10 ppb and a ^{130}Xe lower than for MORB [3]), the resulting ^{238}U/^{130}Xe ratio is even higher than 8.8×10^6 and so the ^{136}Xe/^{130}Xe ratio 3 Ga ago is lower than 2.53. Additionally, ORPC4 #1, which is characterized by the strongest nucleogenic and radiogenic components, show logically the strongest fissiogenic signature (gray circles). The present signature does not reflect the diamond but rather the mineral inclusions. In diagram C, are plotted the ^{131}Xe/^{130}Xe and ^{136}Xe/^{130}Xe ratios for samples of this study (black circles), polycrystalline diamonds from Jwaneng (gray squares [15]), cubic diamonds (gray triangles [5]), fibrous diamonds (gray diamonds [9]) and MORB (black diamonds [35]). For indication, the MORB line defined by the popping rocks is reported [35].

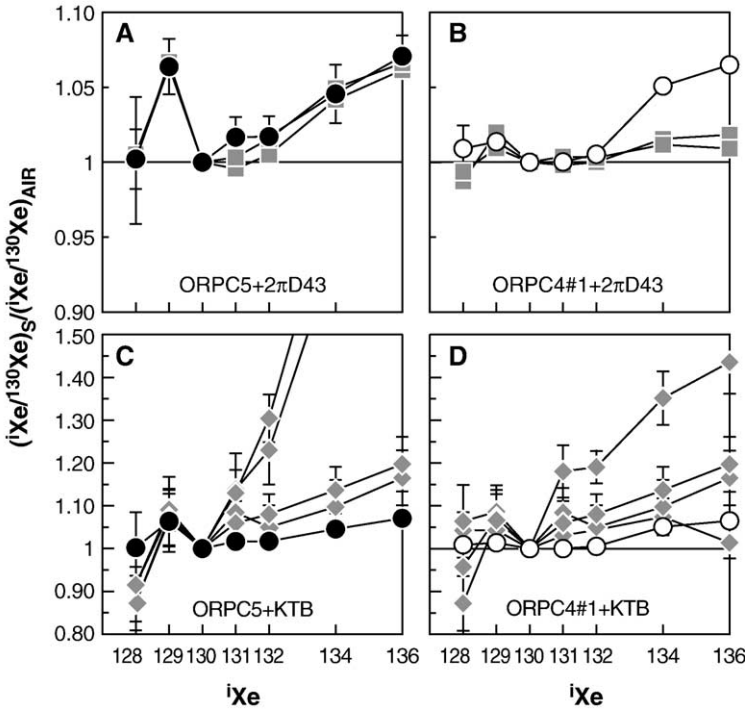

Fig. 4. Xenon isotope patterns for total gas. Diagrams (A and B) respectively represent sample ORPC5 (black circles; characterized by the highest $^{129}Xe/^{130}Xe$ isotopic ratio: 6.91 ± 0.12) and ORPC4 #1 ($^{129}Xe/^{130}Xe = 6.59 \pm 0.04$). For comparison, two steps of the popping rock 2ΠD43 and 2ΠD47 are shown, which have a similar $^{129}Xe/^{130}Xe$ (gray squares; diagram (A): 6.91 ± 0.06; 2ΠD43#6, 50×; 6.93 ± 0.02; 2ΠD43#4, 600 °C; diagram (B): 6.63 ± 0.03; 2ΠD47, 800 °C; 6.56 ± 0.03; 2ΠD43#5, 600 °C [35]). In diagrams (C and D) are reported ORPC5 and ORPC4 #1 and four crustal samples from the KTB drill (showing $^{129}Xe/^{130}Xe$ ranging from 6.93 to 7.09 (diagram C) and from 6.78 to 7.06 (diagram D) [39]). Figures (A and C) clearly show that ORPC5 diamonds are characterized by only similar xenon isotopic signature to the typical MORB source. Additionally, comparison of diagrams (B and D), shows that ORPC4 #1 has an enrichment of fissiogenic xenon compatible with nucleogenic and radiogenic production in the mineral inclusions, rather than a crustal origin of the xenon in the diamonds source.

^{131}Xe anomalies identified among three data by [15] and the contribution of mantle Ne (this study). If the polycrystalline diamonds from Orapa and Jwaneng have a similar origin, then the difference in Ne isotopic signature between this study and those of [15] might be attributed to the method by which the gases were extracted (crushing vs. graphitization).

To check this possibility further, xenon isotopic patterns for two ORPC samples were compared both with mantle and crustal samples (see Fig. 4). Fig. 4A and B compares the results for ORPC5 (characterized by the highest $^{129}Xe/^{130}Xe$ anomaly compared to air) and ORPC4 #1 (characterized by highest nucleogenic Ne and fissiogenic Xe anomalies) with Xe isotopic patterns obtained for popping rocks (a source of reliable upper mantle sampling). In each case, a step was chosen with a $^{129}Xe/^{130}Xe$ close to the diamond value [35]. Similarly, in Fig. 4C and D data from ORPC5 and ORPC4 #1 are reported together with, for comparison, xenon data from the KTB crustal rocks (a reliable continental crust sampling) with similar $^{129}Xe/^{130}Xe$ ratios [39]. Fig. 4A clearly shows that ORPC5 has a xenon isotopic pattern very similar to the upper mantle (MORB). It could be argued that ORPC5 displays a positive ^{131}Xe anomaly (although within error bars of the upper mantle pattern), but this possibility is unlikely, because other diamonds samples as ORPC4 #1 should bear a significant and actually stronger ^{131}Xe anomaly (see Fig. 4B), which is not the case. Thus within the error bar polycrystal-

Table 4
Carbon and nitrogen isotopic ratios and nitrogen concentrations of polycrystalline diamonds from Orapa

Samples	Weight (mg)	$\delta^{13}C‰$	$\delta^{15}N‰$	N (ppm)
ORPC1	0.4697	−14.01	+4.5	202
ORPC2	1.6792	−21.04	+15.5	543
ORPC3	1.4048	−19.37	+6.7	163
ORPC4 #1	1.7067	−9.79	+8.1	1973
ORPC5	1.2141	−18.33	+8.1	69
ORPC6	1.1144	−20.97	+6.7	168

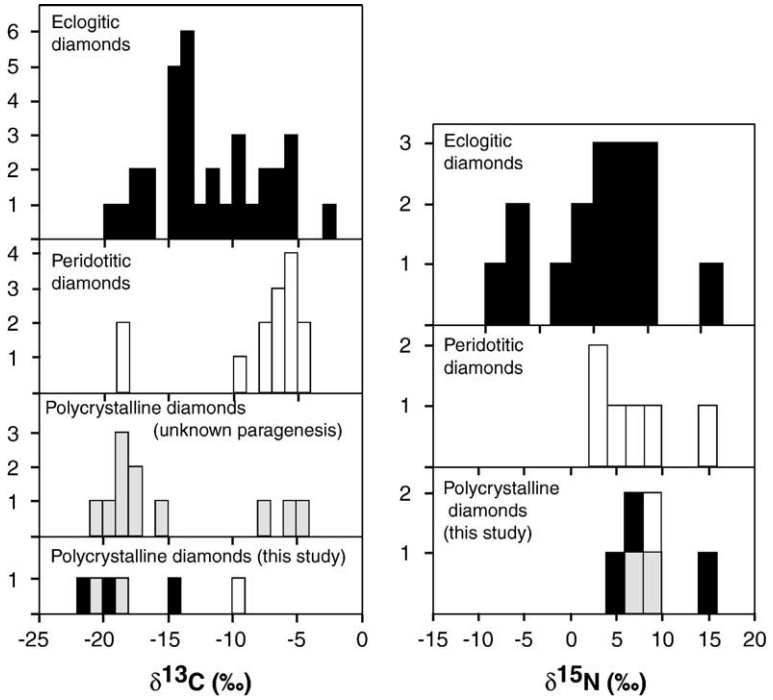

Fig. 5. Histograms illustrating the $\delta^{13}C$ and $\delta^{15}N$ values for both monocrystalline eclogitic and peridotitic diamond and polycrystalline diamonds of unknown paragenesis from Orapa [27] compared with polycrystalline diamonds from the present study.

line diamonds from Orapa show MORB xenon patterns, reflecting their mantle source. Again within errors, the Xe isotopic ratios could indicate a slightly more fissiogenic Xe signature than the MORB mantle source. If correct, this result may reflect Xe fissiogenic production in the parent fluid(s) before diamond crystallization, a view supported by He, Ne, Ar isotopic results, discussed in the following section.

4.2. Origin of the more radiogenic–nucleogenic and fissiogenic component than the MORB mantle source: identification of pre- and post-crystallization processes

The identification within polycrystalline diamonds from Orapa, of a mantle component based on Xe isotopes, which is consistent with the determined Ne data, might mean that other correlations between mantle rare gases can be anticipated. In this section we explore these possibilities and evaluate the likelihood of secondary processes, generating either a radiogenic, nucleogenic, or fissiogenic signature (see [19]).

4.2.1. Helium

The helium isotopic ratios (R/Ra=0.14–1.29, Table 2) indicate the presence of an important radiogenic component in the diamonds (79–98% of He). If this component was secondary, the source could be α-particle implantation from the kimberlite host rocks or from a subsequent secondary source such as α-particle emissions from minerals in an alluvium in which the diamond resides [12]. Alpha particles penetrate the outer 16 μm of a diamond [12], or 30 μm as observed by [40] and, in consequence, there should be a higher ^{4}He* concentration towards the rim of some diamonds. In this regard, the analysis of ORPC4 #1 and ORPC4 #2 (two pieces from the same diamond), the former from the outer part, the latter from the inner part, is of interest. For both pieces, He isotopic ratios are radiogenic, the core (ORPC4 #2, R/Ra=0.14) being more radiogenic than the rim (ORPC4 #1, R/Ra=0.94), which suggests that α-implantation from the host kimberlite is not the main source of radiogenic helium, in this case. In-situ decay of U and Th from production in mineral inclusions [13,14] may be another source of enrichment. Burgess and coworkers [19] calculated a U concentration for polycrystalline diamonds from Orapa of between 24 and 158 ppb, although this value contrasts with U contents of 0.3–1 ppb measured by Kurz et al. ([14] and reference therein). As U and Th are concentrated within mineral inclusions [19,41], a more radiogenic signature should be present either in inclusion-rich diamonds (such as ORPC4 #1) and relatively absent in the 'purest' diamond (such as ORPC 5 or 6). In both cases, no excess

or relative depletion was found in the present data (see Table 2). Thus, neither α-particle bombardment nor in-situ production can adequately account for the total radiogenic helium budget. If the values obtained by Burgess and coworkers [19] are correct, then a third explanation might be that the trapped helium was "already" more radiogenic than subcontinental lithospheric mantle. If the parent fluid(s) were 10 times richer in U, Th than cubic diamonds [19], then over a few million years, such a fluid would bear radiogenic helium.

4.2.2. Neon, argon and xenon

Based on the above discussion, we would expect more nucleogenic Ne, radiogenic Ar and fissiogenic Xe signatures in the parent fluid relative to a representative sample of present-day convective MORB mantle. The occurrence of a "slightly" more nucleogenic Ne isotopic signature within ORPC #6 step 2 (similar to the SCLM) and "slightly" more fissiogenic Xe identified within the sample suite (see Fig. 3B) lends some support to this hypothesis. Thus, we conclude that, the main process accounting for isotopic variability is the post-crystallization nucleogenic, radiogenic and fissiogenic production from U and Th within mineral inclusions, the best example being ORPC4 (Figs. 1–3).

4.3. Elemental rare gas ratios

Rare gas concentrations can provide further insights into diamond post-growth history and growth environment. Fig. 6 compares rare gas concentrations of polycrystalline diamonds to upper mantle abundances and shows that the polycrystalline diamonds are depleted in ^{3}He and ^{22}Ne relative to ^{36}Ar, but that ^{84}Kr and ^{130}Xe show small to negligible depletion. As the mantle-derived rare gases in the polycrystalline diamonds are likely hosted within the same sites, the most likely process to account for the helium and neon depletion seen in Fig. 6 is loss by diffusion.

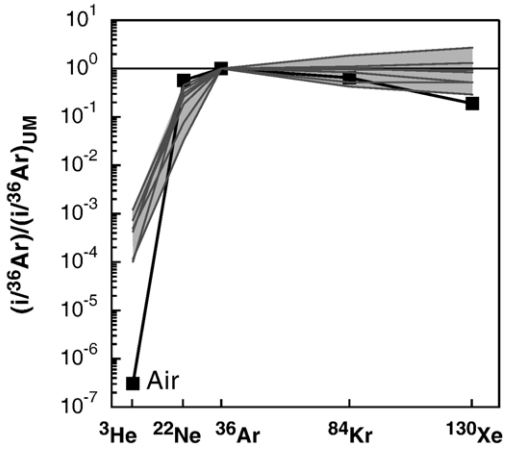

Fig. 6. Rare gas pattern normalized to the upper mantle $(^{i}X/^{36}Ar)_{sample}/(^{i}X/^{36}Ar)_{UM}$; assuming a ^{4}He concentration of 10^{-5} ccSTP/g and rare gas elemental ratio of 7.3, 0.7, 21.3 and 1180 for respectively ^{3}He/^{22}Ne, ^{3}He/^{36}Ar, ^{3}He/^{84}Kr and ^{3}He/^{130}Xe [62]. The ORPC samples are represented within the gray area and the squares stand for the atmospheric pattern.

Further evidence for gas loss is also seen in the ^{4}He/^{40}Ar* ratios, which are characterized by low values of between 0.05 and 1.2 compared to an integrated production ratio ranging between 1.8 (for mantle [42]) and 5 (for continental crust [33]). Low ^{4}He/^{40}Ar* values compared to production ratios are common among mantle xenoliths [43–46] and are interpreted as resulting from helium diffusion [46]. Another explanation, namely that these diamonds crystallize in a high K/U ratio environment, seems improbable because of the required high values of 3.3×10^{4} to 7×10^{5}. The helium diffusion coefficient of diamond (1.9×10^{-16} cm^{2}/s at 1200 °C [13]) means that helium will diffuse about 1cm within a diamond during a 1 Gyr mantle residence time. As the size of the crystallites in these diamonds is a few millimeters, helium can thus diffuse out of the diamond while in the mantle. A second piece of collaborative evidence comes from variations in the ^{22}Ne/^{130}Xe with ^{129}Xe/^{130}Xe ratios (figure not presented) which show that mantle neon was lost and subsequently contaminated by atmospheric neon.

Precise estimates of rare gas losses, however, remain impossible to determine, principally because of late stage atmospheric contamination. Polycrystalline diamonds can be regarded as a porous material (see also [19]) and, although no data are available, the likely sequence for diffusion coefficients of rare gases in diamond is $D_{He}>D_{Ne}>D_{Ar}>D_{Xe}$. If this sequence is correct, then Xe remains the least affected by diffusion.

To have loss of rare gases by diffusion out of diamond, the surrounding mantle must be deprived of those elements. This paradox, namely volatile-rich diamonds stored in volatile-depleted domains, can be understood if polycrystalline diamond grows [47,48] from a volatile (C, N, rare gases)-rich fluid (with a present-day MORB-like rare gases pattern), which intrudes into a rare gas depleted subcontinental lithospheric mantle (SCLM). Such a view is compatible with the proposal that continental lithospheric mantle formed either from the residue after melt extraction (e.g. [49]) or formed by imbrications of recycled material [50], both being depleted in rare gases.

4.4. Polycrystalline diamonds in the integrated models of continental lithosphere evolution: perspectives

The integration of diamond mineral inclusion geochemistry, the carbon and nitrogen isotopes of the host diamond into models of continental lithosphere structure and evolution (e.g. [51]), principally only consider monocrystalline diamonds. Whether the present conclusions inferred from polycrystalline diamond studies can be applied to this more common diamond set, hinges on the precise genetic relationship between the two diamond groups and, for the moment, such a relationship remains unclear. In two extreme cases, monocrystalline and polycrystalline diamonds may crystallize from (1) time unrelated multiple C-bearing fluids derived from distinct carbon sources, or alternatively (2) from a single fluid derived from a single isotopically homogeneous source, different diamond shapes reflecting variations in carbon supersaturation [52] and different C-isotopic compositions resulting from isotope fractionation in the mantle (e.g. [18]).

From present and previous studies [27,28], polycrystalline diamond shows C, N which are unlikely to be related to (kimberlite-related) opaque and/or fibrous cube diamonds, a view contrasting with the suggestion of [53]. Their C and N isotopic compositions are more similar to older xenocrystic monocrystalline diamonds at Orapa. From the present results, the polycrystalline diamonds have similar $\delta^{13}C$ values, but a few slightly extend the range to lower $\delta^{13}C$ values than the monocrystalline diamonds (see Fig. 5). Also the $\delta^{15}N$ values of the polycrystalline diamonds overlap those of the monocrystalline specimens. The present data also show the typical trend of decreasing N concentration with decreasing $\delta^{13}C$ value already identified for both Orapa and worldwide sources [18]. We thus favor crystallization of polycrystalline and monocrystalline diamonds from similar carbon source(s), a suggestion which could be tested by future integrated studies of C, N and rare gases.

According to a coupling between the rare gases, carbon and nitrogen, then such a relationship confines the origin of the carbon. The suggestion that eclogitic diamonds crystallize from recycled metasedimentary carbon was initially based on the recognition that these diamonds more often show $\delta^{13}C$ values below $-10‰$, unlike the majority of peridotitic diamonds [54]. Alternative models involve, for example, isotope fractionation through mineral–fluid reactions controlled by the mineral assemblages of the rocks in which the diamonds formed [18]. Rare gases are minor volatile components of mantle fluids/melts having, for example, C/He ratios of $>10^4$ [55]. The present evidence of mantle-derived He–Ne–Ar and Xe isotopic compositions among polycrystalline diamonds from Orapa although associated with low $\delta^{13}C$ values (from -9 down to $-22‰$), therefore, point to the occurrence for an associated mantle-derived origin of their carbon. As mantle-derived rare gases are observed within both eclogitic and peridotitic diamonds, these observations contradict models that suggest eclogitic and peridotitic diamonds have distinct carbon sources. In the light of the present mantle Xe evidence, unusual carbon isotope variations are therefore best explained as resulting from isotope fractionation through mineral–fluid reactions controlled by the mineral assemblages of the rocks in which the diamonds formed [18].

4.5. Origin of the Xenon signature and "Xenon ages" of diamonds?

Several xenon isotopes ($^{131,132,134,136}Xe$) were created after Earth accretion by fission of extinct ^{244}Pu (half life of ^{82}Ma, i.e. no contribution since 3.4–3.5 Ga [56]) and by the spontaneous fission of the ^{238}U (half life of 4.47 Ga). The contribution of $^{131–136}Xe$ production is not equal for each isotope depending on its branching ratio [56–58]. Thus, the combination of the $^{131}Xe/^{130}Xe$, $^{132}Xe/^{130}Xe$, $^{134}Xe/^{130}Xe$ and $^{136}Xe/^{130}Xe$ ratios can constrain the relative contributions of ^{244}Pu and ^{238}U [35,59]. For Archean samples such as diamonds (3.2 to 1 Ga; for review see [51]) which includes eclogitic diamonds from Orapa (2.9 to 1 Ga [4,51]), the evolution of the $^{131–136}Xe$, if detectable, could allow age constraints to be placed on the timing of diamond formation.

As xenon isotopic evolution through time is poorly documented [35], we will only consider the most constrained $^{136}Xe/^{130}Xe$ and $^{129}Xe/^{130}Xe$ ratios. Assuming a closed system, evolution of the $^{136}Xe/^{130}Xe$ ratio can be calculated, if $^{136}Xe/^{130}Xe$ originates from the spontaneous fission of ^{238}U (for the equation, see [34]). For the polycrystalline diamonds from Orapa (both eclogitic and peridiotitic) this ratio varies between 2.17 and 2.34. In addition, it is interesting to note that similar Xe isotope results were obtained by [9] on coated monocrystalline diamonds, assuming core ages between 1.8 and 3.2 Ga and a coat age of about 100 Ma. Data for cube diamonds [5], that may have been formed just before kimberlite eruption (in this case about 77 Ma ago), also show xenon ratios similar to the previous diamond studies. Available data suggests, therefore, that whatever the published age of diamonds, their xenon isotopic ratios indicate that diamonds have xenon signatures ranging from present-

day mantle to only slightly more fissiogenic. This conclusion may imply that (1) the mantle Xe isotopic ratios have not evolved since diamond crystallization (because no detectable fissiogenic Xe from fission of ^{238}U exists in the mantle), or (2) that diamonds could be much younger in age and percolation of mantle xenon, from the asthenosphere through the subcontinental lithosphere occurred, as previously suggested for helium [3].

5. Conclusions

He, Ne, Ar and Xe isotopic compositions measured in eclogitic, peridotitic and unknown paragenesis polycrystalline diamonds from Orapa require the presence of a mantle component in the source of the diamonds, there being no need to call for a crustal origin. This implies an associated mantle-derived origin of the diamond carbon.

The parent fluid(s) of polycrystalline diamonds was likely enriched in incompatible elements such as U, Th and K leading to a time-integrated more radiogenic–nucleogenic and fissiogenic rare gas signature than for (kimberlite-related) cubic diamonds.

In addition, post-crystallization radioactive decay of thorium, uranium and potassium results in the production of radiogenic-nucleogenic and fissiogenic helium, neon, argon and xenon affecting the trapped rare gas signature. Finally, the rare gases diffuse out of the diamonds to a degree, inversely proportional to their atom sizes. Xenon is less affected by this process.

Therefore, polycrystalline diamonds are not the best samples to constrain the rare gas history of the mantle throughout time but give important information about fluid origin, composition and post-crystallization processes. The fact that xenon isotopic ratios preserve a signature similar to present-day MORB mantle xenon (this result being supported by available data on all other diamonds) suggests that the diamonds are either (1) much younger than 1 Ga or (2) that the mantle $^{136}Xe/^{130}Xe$ ratio is frozen since diamonds crystallization, 3.2 Ga ago.

Acknowledgements

We thank the DeBeers Group of Companies for the donation of the samples. Philippe Sarda is warmly thanked for all the comments and discussions at different stages of the manuscript. Bernard Bourdon and David Shuster are thanked for their critical comments. We also thank Emilie Thomassot for the meaningful discussions. The quality of the manuscript was strongly improved by the constructive reviews of Pete Burnard and an anonymous reviewer.

References

[1] C.J. Allègre, M. Moreira, T. Staudacher, $^{4}He/^{3}He$ dispersion and mantle convection, Geophys. Res. Lett. 22 (17) (1995) 2325–2328.
[2] C.J. Allègre, E. Lewin, Isotopic systems and stirring times of the Earth's Mantle, Earth Planet. Sci. Lett. 136 (1995) 629–646.
[3] C.E. Gautheron, M. Moreira, Helium signature of the subcontinental lithospheric mantle, Earth Planet. Sci. Lett. 199 (2002) 39–47.
[4] S.H. Richardson, J.W. Harris, J.J. Gurney, Three generations of diamonds from old continental mantle, Nature 366 (1993) 256–258.
[5] N. Wada, J. Matsuda, A noble gas study of cubic diamonds from Zaire: constraints on their mantle source, Geochim. Cosmochim. Acta 62 (1998) 2335–2345.
[6] S.R. Boyd, F. Pineau, M. Javoy, Modeling the growth of natural diamonds, Chem. Geol. 116 (1994) 29–42.
[7] T. Akagi, A. Masuda, Isotopic and elemental evidence for relationship between kimberlite and Zaire cubic diamonds, Nature 336 (1988) 665–667.
[8] M. Ozima, S. Zashu, O. Nitoh, $^{3}He/^{4}He$ ratio, noble gas abundance and K-Ar dating of diamonds—an attempt to search for the records of early terrestrial history, Geochim. Cosmochim. Acta 47 (1983) 2217–2224.
[9] M. Ozima, S. Zashu, Noble gas state of the ancient mantle as deduced from noble gases in coated diamonds, Earth Planet. Sci. Lett. 105 (1991) 13–27.
[10] M. Ozima, F.A. Podozek, G. Igarashi, Terrestrial xenon isotope constraints on the early history of the Earth, Nature 315 (1985) 471–474.
[11] G. Kurat, G. Dobosi, Garnet and diopsite-bearing diamondites (framesites), Mineral. Petrol. 69 (2000) 143–159.
[12] D. Lal, An important source of ^{4}He (and ^{3}He) in diamonds, Earth Planet. Sci. Lett. 96 (1989) 1–7.
[13] R.C. Weins, D. Lal, W. Rison, J.F. Wacker, Helium isotope diffusion in natural diamonds, Geochim. Cosmochim. Acta 58 (7) (1994) 1747–1757.
[14] M.D. Kurz, J.J. Gurney, W.J. Jenkins, D.E. Lott III, Helium isotopic variability within single diamonds from the Orapa kimberlite pipe, Earth Planet. Sci. Lett. 86 (1987) 57–68.
[15] M. Honda, D. Phillips, J.W. Harris, I. Yatsevich, Unusual noble gas compositions in polycrystalline diamonds: preliminary results from the Jwaneng kimberlite, Botswana, Chem. Geol. 203 (2004) 347–358.
[16] G.L. Davis, The age and uranium contents of zircons from kimberlites and associated rocks, Carnegie Inst. Wash, Yearbook 76 (1977) 631–635.
[17] S.R. Boyd, R.-M.A., M. Javoy, Improved techniques for the extraction, purification and quantification of nanomole quantities of nitrogen gas: the nitrogen content of a diamond, Meas. Sci. Technol. 6 (1995) 297–305.
[18] P. Cartigny, J.W. Harris, M. Javoy, Diamond genesis, mantle fractionations and mantle nitrogen content: a study of $\delta^{13}C$–N concentrations in diamonds, Earth Planet. Sci. Lett. 185 (2001) 85–98.
[19] R. Burgess, L.H. Johnson, D.P. Mattey, J.W. Harris, G. Turner, He, Ar and C isotopes in coated and polycrystalline diamonds, Chem. Geol. 146 (1998) 205–217.
[20] M. Ozima, S. Zashu, Solar-type Ne in Zaire cubic diamonds, Geochim. Cosmochim. Acta 52 (1988) 19–25.

[21] M. Ozima, F.A. Podosek, Noble Gas Geochemistry, New York, 1983, 367 pp.
[22] P. Sarda, T. Staudacher, C.J. Allègre, Neon isotopes in submarine basalts, Earth. Planet. Sci. Lett. 91 (1988) 73–88.
[23] M. Honda, I. McDougall, D.B. Patterson, A. Doulgeris, D. Clague, Possible solar noble-gas component in Hawaiian basalts, Nature 349 (1991) 149–151.
[24] H. Hiyagon, M. Ozima, B. Marty, S. Zashu, H. Sakai, Noble gases in submarine glasses from mid-oceanic ridges and Loihi seamount: constraints on the early history of the Earth, Geochim. Cosmochim. Acta 56 (1992) 1301–13016.
[25] M. Moreira, K. Breddam, J. Curtice, M. Kurz, Solar neon in the Icelandic mantle: evidence for an undegassed lower mantle, Earth Planet. Sci. Lett. 185 (2001) 15–23.
[26] E. Dixon, M. Honda, I. McDougall, I. Campbell, I. Sigurdsson, Preservation of near-solar isotopic ratios in Icelandic basalts, Earth Planet. Sci. Lett. 180 (2000) 309–324.
[27] P. Deines, J.W. Harris, J.J. Gurney, Depth-related carbon isotope and nitrogen concentration variability in the mantle below the Orapa Kimberlite, Botswana, Africa, Geochim. Cosmochim. Acta 57 (1993) 2781–2796.
[28] P. Cartigny, J.W. Harris, M. Javoy, Eclogitic, Peridotitic and Metamorphic diamonds and the problems of carbon recycling—the case of Orapa (Botswana), 7th Int. Kimberlite Conf. 1, Red Roof Design, 1999, pp. 117–124.
[29] W. Kaiser, W.L. Bond, Nitrogen, a major impurity in common type I diamond, Phys. Rev. 115 (4) (1959) 857–863.
[30] P. Cartigny, Early Proterozoic Ultrahigh pressure metamorphism: evidence from microdiamonds, Science 304 (2004) 853–855.
[31] R. Burgess, G.B. Kiviets, J.W. Harris, Ar-Ar age determinations of eclogitic clinopyroxene and garnet inclusions in diamonds from the Venetia and Orapa kimberlites, Lithos 77 (2004) 113–124.
[32] D. Phillips, J.W. Harris, G.B. Kiviets, $^{40}Ar/^{39}Ar$ analyses of clinopyroxene inclusions in African diamonds: implications for source ages of detrital diamonds, Geochim. Cosmochim. Acta 68 (2004) 151–165.
[33] C.J. Ballentine, P.G. Burnard, Production, release and transport of noble gases in the continental crust, in: C.J.B.D. Porcelli, R. Wieler (Eds.), Noble Gases Geochemistry and Cosmochemistry, Reviews in Mineralogy and Geochemistry, vol. 47, 2002.
[34] T. Staudacher, C.J. Allègre, Terrestrial xenology, Earth Planet. Sci. Lett. 60 (1982) 389–406.
[35] J. Kunz, T. Staudacher, C.J. Allègre, Plutonium–fission xenon found in Earth's mantle, Science 280 (1998) 877–880.
[36] T. Bernatowicz, J. Brannon, R. Cowsik, C.M. Hohenberg, F.A. Podosek, Precise determination of relative and absolute $\beta\beta$ decay rates of ^{128}Te and ^{130}Te, Phys. Rev. C47 (1993) 806–825.
[37] J.C. Browne, B.L. Berman, Neutron capture cross-sections for ^{128}Te and ^{130}Te and the xenon anomaly in old tellurium ores, Phys. Rev. C8 (1973) 2405–2411.
[38] D.L. Pinti, J.-I. Matsuda, S. Maruyama, Anomalous xenon in Archean cherts from Pilbara Craton, Western Australia, Chem. Geol. 175 (2001) 387–395.
[39] J. Drescher, T. Kirsten, K. Schäfer, The rare gas inventory of the continental crust, recovered by the KTB Continental Deep Drilling project, Earth Planet. Sci. Lett. 154 (1998) 247–263.
[40] D.A. Shelkov, A.B. Verchovsky, H.J. Milledge, C.T. Pillinger, The radial distribution of implanted and trapped ^{4}He in single diamond crystals and implications for the origin of carbonado, Chem. Geol. 149 (1998) 109–116.
[41] J.D. Kramers, Lead, Uranium, Strontium, Potassium and Rubidium in inclusion-bearing diamonds and mantle derived xenoliths from Southern Africa, Earth Planet. Sci. Lett. 42 (1979) 58–70.
[42] D. Graham, Noble gas isotope geochemistry of mid-ocean ridge and ocean island basalts: characterization of mantle source reservoirs, in: C.J.B.D. Porcelli, R. Wieler (Eds.), Noble Gases in Geochemistry and Cosmochemistry, Reviews in Mineralogy and Geochemistry, vol. 47, 2002, pp. 247–317.
[43] T.J. Dunaï, H. Baur, Helium, neon and argon systematics of the European subcontinental mantle: implications for its geochemical evolution, Geochim. Cosmochim. Acta 59 (1995) 2767–2783.
[44] T. Matsumoto, M. Honda, I. McDougall, S. O'Reilly, Noble gases in anhydrous lherzolites from the Newer Volcanics, southeastern Australia: a MORB-like reservoir in the subcontinental mantle, Geochim. Cosmochim. Acta 62 (1998) 2521–2533.
[45] T. Matsumoto, M. Honda, I. McDougall, S.Y. O'Reilly, M. Norman, G. Yaxley, Noble gases in pyroxenites and metasomatised peridotites from the Newer Volcanics, southeastern Australia: implications for mantle metasomatism, Chem. Geol. 168 (2000) 49–73.
[46] C. Gautheron, M. Moreira, C.J. Allègre, He, Ne and Ar composition of the European lithospheric mantle, Chem. Geol. 217 (2005) 97–112.
[47] J.J. Gurney, F.R. Boyd, Intergrowths with polycrystalline diamonds from the Orapa Mine, Botswana, Yb. Carnegie Inst, (1982) 267–273.
[48] D.E. Jacob, K.S. Viljoen, N. Grassineau, J.E., Remobilization in the Cratonic lithosphere recorded in polycrystalline diamonds, Science 289 (2000) 1182–1185.
[49] C. Herzberg, Phase equilibrium constraints on the formation of cratonic mantle. In Mantle petrology: field observations and high pressure experimentation, The Geochemical Society Spec. 6 (1999) 241–258.
[50] H. Helmstaedt, R. Doig, Eclogite nodule from kimberlite pipe in the Colorado plateau. Samples of subducted Franciscan type oceanic lithosphere, Phys. Chem. Earth 9 (1975) 95–111.
[51] S.B. Shirey, J.W. Harris, S.H. Richardson, M.J. Fouch, D.E. James, P. Cartigny, P. Deines, F. Viljoen, Diamond genesis, seismic structure, and evolution of the Kaapvaal–Zimbabwe Craton, Science 297 (2002) 1683–1686.
[52] I. Sunagawa, Growth and morphology of diamond crystals under stable and metastable conditions, J. Cryst. Growth 99 (1990) 1156–1161.
[53] P.J. Heaney, E.P. Vicenzi, S. De, Strange diamonds: the mysterious origins of carbonado and framesite, Elements 1 (2) (2005) 85–89.
[54] N.V. Sobolev, E.M. Galimov, I.N. Ivanovskaya, E.S. Yefimova, Isotope composition of carbon in diamonds containing crystalline inclusions, Dokl. Akad. Nauk SSSR 249 (1979) 1217–1220.
[55] B. Marty, A. Jambon, $C/^{3}He$ in volatile fluxes from the solid Earth: implications for carbon geodynamics, Earth Planet. Sci. Lett. 83 (1979) 16–26.
[56] P.R. Fields, A.M. Friedman, J. Milsted, J. Lerner, C.M. Stevens, D. Metta, W.K. Sabine, Decay properties of plutonium-244, and comments on its existence in nature, Nature 212 (5058) (1966) 131–134.
[57] A.H. Jaffey, K.F. Flynn, L.E. Glendenin, W.C. Bentley, A.M. Essling, Precision measurements of half-lives and specific activities of ^{235}U and ^{238}U, Phys. Rev. C4 (1971) 1889–1906.
[58] J.M. Roberts, R. Gold, R.J. Armani, Spontaneous fission decay of ^{238}U, Phys. Rev. 174 (1968) 1482–1484.

[59] M. Honda, A.P. Nutman, V.C. Bennett, Xenon compositions of magmatic zircons in 3.64 and 3.81Ga meta-granitoids from Greenland- a search for extinct ^{244}Pu in ancient terrestrial rocks, Earth Planet. Sci. Lett. 207 (2003) 69–82.
[60] B.M. Kennedy, H. Hiyagon, J.H. Reynolds, Crustal neon: a striking uniformity, Earth Planet. Sci. Lett. 98 (1990) 277–286.
[61] C.J. Allègre, T. Staudacher, P. Sarda, Rare gas systematics, formation of the atmosphere, evolution and structure of the Earth's mantle, Earth Planet. Sci. Lett. 81 (1986/87) 127–150.
[62] M. Moreira, J. Kunz, C.J. Allègre, Rare gas systematics in popping rock: isotopic and elemental compositions in the upper Mantle, Science 279 (1998) 1178–1181.